

Explaining the presence of perennial liquid water bodies in the firn of the Greenland Ice Sheet

P. Kuipers Munneke,¹ S. R. M. Ligtenberg,¹ M. R. van den Broeke,¹

J. H. van Angelen,¹ and R. R. Forster²

¹Institute for Marine and Atmospheric research, Utrecht University, Utrecht, The Netherlands.

²Department of Geography, University of Utah, Salt Lake City, UT, USA.

This article has been accepted for publication and undergone full peer review but has not been through the copyediting, typesetting, pagination and proofreading process, which may lead to differences between this version and the Version of Record. Please cite this article as doi: 10.1002/2013GL058389

Recent observations have shown that the firn layer on the Greenland ice sheet features subsurface bodies of liquid water at the end of the winter season. Using a model with basic firn hydrology, thermodynamics, and compaction in one dimension, we find that a combination of moderate to strong surface melt and a high annual accumulation rate is required to form such a perennial firn aquifer. The high accumulation rate ensures that there is pore space available to store water at a depth where it is protected from the winter cold. Low-accumulation sites cannot provide sufficiently deep pore space to store liquid water. However, for even higher accumulation rates, the total cold content of the winter accumulation becomes sufficient to refreeze the total amount of liquid water. As a consequence, winter- or springtime observations of subsurface liquid water in these specific accumulation conditions cannot distinguish between a truly perennial firn aquifer and water layers that will ultimately refreeze completely.

1. Perennial firn aquifers

Recently, the existence of large areas with liquid water present within the firn layer of the Greenland ice sheet at the end of winter has been demonstrated by ground penetrating radar, airborne radar, and firn cores [Forster *et al.*, 2013; Koenig *et al.*, 2013]. With the discovery of these perennial firn aquifers, a new way of liquid water storage was identified. Previously, the possibility of liquid water persisting within the upper ~10 m of the snow/firn during winter was suspected [Humphrey *et al.*, 2012] and the potential for liquid or refrozen meltwater stored in firn pore space throughout the percolation zone of the entire ice sheet was identified [Harper *et al.*, 2012]. The existence of firn aquifers may have an impact on our understanding of the water and energy budget of the ice sheet: a subsurface volume of liquid water represents a significant pool of latent energy, that needs to be refrozen before the firn layer can start to cool below the freezing point. This latent heat in the ice sheet is no longer needed if future atmospheric warming starts to melt the firn layers containing the aquifer.

Observations of firn aquifers are mostly confined to the southeastern part of the Greenland Ice Sheet, where short-lived supraglacial meltwater lakes are almost completely absent [Selmes *et al.*, 2011]. It is conceivable that the presence of a thick firn layer in which an aquifer can form precludes the widespread annual recurrence of these supraglacial lakes, although this would need to be investigated further. In addition, water in the aquifers does not enter the englacial and subglacial hydrological system directly. Thus, the response of firn-aquifer regions to surface warming is likely different from non-aquifer regions, in at least two ways: (1) the paucity of supraglacial lakes and streams changes the feedback

between melt and surface albedo, and (2) the lack of a direct connection between surface meltwater and the subglacial hydrological system inhibits or lags an impact of meltwater production on the ice dynamics. It is therefore interesting to investigate how, and under what conditions, firn aquifers form. A consistent physical explanation for the formation of firn aquifers has not been provided yet.

In this study, we use a one-dimensional firn model that includes compaction, basic meltwater hydrology, and thermodynamics, to understand the mechanisms responsible for the formation of firn aquifers. To understand what climatic conditions are required for these firn aquifers to develop, we prescribe a simple surface climate that is defined in terms of accumulation and surface temperature only.

2. Firn model essentials

The firn model is described in *Ligtenberg et al.* [2011]. The essential physics of this model are presented below. The model consists of layers of varying thickness in a Lagrangian setting, i.e. the properties of each layer (temperature, mass, density, liquid water content) are tracked together with the layer as it moves down into the firn pack. To ensure numerical stability, the minimum layer thickness is 4.5 cm. Whenever a layer exceeds a thickness of 10.5 cm, the layer is split into two equally thick layers, which inherit the properties of their parent layer. Whenever a layer becomes thinner than 4.5 cm (e.g. due to compaction or surface melt), the layer is merged with the neighbouring one, and the properties of the merged layer are taken as a mass-weighted mean of the two parent layers.

2.1. Density and compaction

The density of freshly fallen snow is taken constant at 300 kg m^{-3} . Dry firn compaction is adapted from *Arthern et al.* [2010], who expresses the change in snow density ρ as a function of time t :

$$\frac{d\rho}{dt} = MO \cdot C \dot{b} g (\rho_i - \rho) e^{-\frac{E_c}{RT} + \frac{E_g}{RT}}, \quad (1)$$

where \dot{b} is accumulation rate, ρ_i is the density of glacial ice, g , E_c , E_g , and R are constants, and T is temperature in K. To reflect the higher densification rate for low-density firn, the value of C is 0.07 for $\rho < 550 \text{ kg m}^{-3}$ and 0.03 for $\rho \geq 550 \text{ kg m}^{-3}$. *Ligtenberg et al.* [2011] employed Eq. 1 and compared the resulting modelled firn density profiles to 48 firn cores, to find that Eq. 1 requires a multiplication factor MO that depends on the accumulation rate \dot{b} :

$$MO = \alpha - \beta \ln(\dot{b}), \quad (2)$$

where $\{\alpha, \beta\} = \{1.435, 0.151\}$ for $\rho < 550 \text{ kg m}^{-3}$, and $\{2.366, 0.293\}$ for $\rho \geq 550 \text{ kg m}^{-3}$.

2.2. Hydrology

Surface meltwater (which is assumed to be a function of surface temperature, see section Model Strategy) percolates into the firn, where it refreezes in any subsurface layer that is below the freezing point. The release of latent heat upon refreezing heats up the layer in which the water refreezes, ensuring that energy is conserved in the firn column. The maximum capillary water storage capacity of the layer W_c (in mass-% of the entire layer) is a function of its density, following *Coléou and Lesaffre* [1998]:

$$W_c = 1.7 + 5.7 \frac{P}{1 - P}. \quad (3)$$

Here, P is the firn porosity defined as $P = 1 - (\rho/\rho_i)$. In this way, the liquid water capacity W_c of a layer decreases as its density increases. If meltwater encounters a layer in which the maximum storage capacity of capillary water is reached (i.e. with a water content equalling W_c), the meltwater percolates down to the first layer where the capillary capacity is unsaturated. This approach is known as a tipping-bucket method, in which water tips from one layer to the next until it finds a place to be stored. It equals the description of homogeneous wetting front motion, with the additional conditions that (a) saturation beyond the capillary storage capacity of layers is never allowed, and that (b) the vertical displacement of meltwater occurs in a single time step. Finally, when meltwater reaches the firn-ice interface, we assume that it will leave the firn column as runoff instantaneously. This assumption likely leads to a faster drainage than what is suspected from observations: we will come back to this in the discussion.

2.3. Thermodynamics

The thermodynamical part of the firn model consists of two parts. The first part describes the conduction of heat following a one-dimensional time-dependent heat-transfer equation. The second part computes the heat released upon refreezing of meltwater in the firn pack. Because of the Lagrangian setup of the model, vertical advection of heat is automatically taken into account. As a basal boundary condition, the temperature of the lowermost model layer is set by the spin-up procedure as the result of vertical advection and diffusion of heat.

2.4. Model strategy

The surface climate is defined by three variables only: \dot{b} , T_a and ΔT , which represent annual accumulation (mm w.e. y^{-1}), mean annual surface temperature ($^{\circ}\text{C}$), and amplitude of a sinusoidal annual cycle of surface temperature T ($^{\circ}\text{C}$), respectively. Surface temperature peaks in July and reaches a minimum in January (see figure 1a). Surface melt M (mm w.e. day^{-1}) is made a function of surface temperature using the simplest form of the positive degree-day (PDD) formulation [Braithwaite, 1985]:

$$M = DDF_s \sum (T - T_0) \Delta t, \quad (4)$$

where DDF_s is a degree-day factor (mm w.e. $\text{day}^{-1} \text{ }^{\circ}\text{C}^{-1}$), T_0 is a threshold temperature for melting, and Δt is a period of time. *Van den Broeke et al.* [2010] demonstrated that the following values give good results over much of Greenland when using daily mean temperature: $DDF_s = 1.5 \text{ mm w.e. } \text{day}^{-1} \text{ }^{\circ}\text{C}^{-1}$, and $T_0 = -5^{\circ}\text{C}$.

Furthermore, the annual accumulation rate \dot{b} is assumed constant throughout the year, and the temperature of fresh snow is equal to the surface temperature. The surveyed parameter space has the following bounds: $100 \leq \dot{b} \leq 5000 \text{ mm w.e. } y^{-1}$; $-22 \leq T_a \leq -12^{\circ}\text{C}$; and $9 \leq \Delta T \leq 20^{\circ}\text{C}$. We restricted the parameter space further, to temperature conditions that are observed at the present-day Greenland ice sheet: this excludes mean July temperatures $> 1^{\circ}\text{C}$. Moreover, we have only sampled the part of this 3-D parameter space that results in surface melting, i.e. to those temperature curves for which $T > T_0$ at some point during the year. A schematic overview of the parameter space in the $\{T_a, \Delta T\}$ -plane is shown in 1b.

To achieve a firn layer that is in equilibrium with its surface climate, the model is first spun up. The required spin-up time is calculated as the total thickness of the modelled firn layer divided by the annual accumulation [Ligtenberg *et al.*, 2011]. In this way, the entire firn column is refreshed once at the end of the spin-up time. The total firn-layer thickness is not prescribed, but always such that it includes the depth at which the ice density is reached (sometimes up to 150 m) after the spin-up procedure. After spin-up, the model is run for three more years to generate sufficient output to study the annual cycle.

3. Results

Unlike other temporary bodies of liquid water in the firn, a perennial firn aquifer persists throughout the winter season. They are potentially replenished at the start of the melting season of the following year. To assess whether a firn aquifer is present, we look at the vertically integrated liquid water mass (total liquid water, in mm) at the end of winter, on the 1st of March. In Fig. 2, 11 cross sections of the entire parameter space are presented, with one panel for each 1°C interval of T_a , annual accumulation \dot{b} on the horizontal axes, and ΔT on the vertical axes.

It is clear that perennial water starts to form in appreciable quantities for combinations of high T_a and high ΔT , which corresponds to conditions with high melt fluxes. Therefore, the presence of a firn aquifer is determined by the amount of surface melt, with higher melt rates corresponding to more perennial water.

The presence of a firn aquifer also depends on the accumulation rate (Fig. 2). For a given T_a and ΔT , the amount of liquid water first increases as the accumulation rate

increases; however, above a certain accumulation rate, this relation is reversed, and the amount of liquid water starts to decrease for increasing accumulation rate. Thus, there exists an accumulation rate for which the vertically integrated amount of liquid water has a maximum.

We explore this behaviour by looking at the time evolution of liquid water, density, and firn temperature in three firn columns with an identical temperature (and thus melt) forcing, but different accumulation rate (see Fig. 3). The annual melt is slightly over 200 mm w.e. y^{-1} in all three cases. For a relatively low accumulation rate of 500 mm w.e. y^{-1} (Fig. 3a,d,g), the liquid water formed by summer melting, is refrozen within a period of 1 or 2 months after the melt season has ended. Because of the low accumulation rate, the firn layer is shallow and the density high. There is little pore space in the firn because the supply of pore space (by fresh snow) is small, and the pore space is further reduced by refreezing of meltwater. Because there is little pore space available in the firn, only little meltwater can be accommodated. Below 7–8 m beneath the surface, solid ice is encountered (identified as a high-density layer). For liquid water, it means that most meltwater leaves the firn as runoff. The remaining amount of liquid water is sufficiently small to be refrozen quickly.

For an accumulation rate of 1750 mm w.e. y^{-1} (Fig. 3b,e,h), there is more pore space available in which to store liquid water. The amount of liquid water that needs to be refrozen at the end of summer is therefore also greater. Moreover, pore space is available sufficiently deep to isolate the liquid water from the winter cold. Or stated differently: the rate at which the liquid layer is refrozen from above is not high enough to prevent

the firn aquifer to be recharged by meltwater in the next melt season. As a result, liquid water remains in the firn pack perennially. In the example in Fig. 3b, the upper boundary of the firn aquifer is situated approximately 10 m below the surface.

When the accumulation rate equals 4500 mm w.e. y^{-1} (Fig. 3c,f,i), all the liquid water is eventually refrozen in the course of the next melt season, at a depth of about 14 m below the surface. We explain this as follows: the total refreezing capacity of the firn is ultimately determined by the total cold content provided by snowfall. This cold content is linearly proportional to the accumulation rate. For the example in Fig. 3b ($\dot{b} = 1750$ mm w.e. y^{-1}), the cold content of the winter layer is insufficient to refreeze the summer wet layer completely. As a result, the liquid water remains in the firn perennially. In the example of Fig. 3c ($\dot{b} = 4500$ mm w.e. y^{-1}), the total cold content of the winter layer becomes so large that the summer wet layer is refrozen eventually. It is done so by diffusion of released latent heat away from the refreezing wet layer towards the dry and cold winter snow. The refreezing process takes about one full year in the example in Fig. 3c. Interestingly, this configuration does not lead to a perennial firn aquifer in the sense that there is a permanently liquid layer present below the surface. However, liquid water will be encountered in the firn throughout the year because the refreezing of the wet layer originating from one summer continues into the next summer season. We refer to this situation as a pseudo-perennial firn aquifer. When probing the firn layer (either in-situ or using remote sensing techniques), no distinction is possible between a perennial and a pseudo-perennial firn aquifer. Hence, one should be careful not to conclude the perennial

presence of meltwater based on a winter- or springtime observation of liquid water only, in these specific temperature and accumulation conditions.

To look at the firn aquifer in more detail, we show the temporal evolution of liquid water, density, and temperature of a firn layer in which a firn aquifer is present in Fig. 3b, e, and h. At the start of the melt season (around May in this example), the refreezing of percolating meltwater brings the first 10 m of the firn column to the melting point within 3 months. The refrozen meltwater also increases the density. The density in the isothermal summer firn column is further increased as a consequence of the higher densification rate that is associated with higher firn temperature. Because the capillary capacity of firn decreases with increasing density, the liquid water is ‘squeezed’ out of the firn and percolates further down the firn column. This explains the gradual decrease of the liquid water content in a layer that is being buried during summer. After the melt season (end of August in this example), the liquid layer is being buried under snow that is below the melting point. This enables refreezing of the wet summer layers from above. However, in this case the entire wet layer cannot be refrozen before it is recharged in the next melt season, and thus, the liquid water in this layer continues to exist throughout the year. When probing this particular firn layer in March, the horizon of wet firn would be found around 8 m depth. The firn below 10 m depth is isothermal (at the melting point) throughout the year, and contains a perennial water body.

How well does the model predict the existence of firn aquifers in the Greenland Ice Sheet? To answer this question, we use 1960–2012 mean annual accumulation, temperature, and temperature amplitude from the regional climate model RACMO2 [*Van Angelen et al.*,

2012]. We use these three parameters as predictors for the liquid water content at the end of winter, according to the simple firn model. If we use half the difference between the mean January and July temperature as the temperature amplitude ($\Delta T_{RACMO} = (T_{Jul} - T_{Jan})/2$, Fig. 4a), we see very few locations on the Greenland Ice Sheet that feature a firn aquifer (Fig. 4d). The reason is that the real annual temperature cycle is flattened in summer because the melting surface cannot raise its temperature above the melting point. Using the real cycle in the simple model thus gives a temperature amplitude that is too low. As an alternative, we took the wintertime amplitude ($\Delta T_{RACMO} = (T_{May} + T_{Sep})/2 - T_{Jan}$, Fig. 4b) as a predictor, leading to the map of liquid water content in March as shown in Fig. 4c. This panel also shows all Operation Ice Bridge radar flight lines carried out in 2011 [Forster *et al.*, 2013], and the locations where an aquifer was detected are shown in the inset in Fig. 4e as black dots. Both the observations and the parameterized liquid water content show an abundance of firn aquifers in the southeastern part of the Greenland Ice Sheet, and to a lesser extent in the percolation zone above 2000 m a.s.l. in the southwest. The model and the observations also agree on a complete absence of firn aquifers in the western, northern, and eastern parts of the ice sheet.

4. Discussion, implications, and conclusions

We have formulated a deliberately simple firn model forcing that still explains the formation of firn aquifers. The results of this study may change quantitatively when a more complex model formulation is chosen, or when a more realistic surface climate forcing is prescribed. As an example of the latter, the PDD-relation between temperature and melt is a simplification of the true response of a melting snow surface to temperature

change. A more sophisticated computation of surface melt in an idealised climate may reveal a higher or lower sensitivity of melt flux to temperature. Also, the above-mentioned summertime flattening of the real annual temperature cycle has implications for the annual melt rate associated with the values of T_a and ΔT presented here. The use of the winter temperature amplitude (as above) can solve this problem. Another issue is that high-accumulation sites often receive most snowfall during the winter. Thus, our assumption of a constant accumulation rate may underestimate both the winter cold content and the depth of the firn aquifer at the end of winter.

As a key example of simple model formulation, the firn model does not account for heterogeneous vertical motion of meltwater, a process generally referred to as piping or preferential flow [Benson, 1962; Marsh and Woo, 1984]. Piping occurs as a consequence of instabilities that develop as the wetting front moves downward through the firn at the start of the melt season. The emerging pipes carry water down through the firn while the surrounding firn is not at the melting point. In this way, the requirement that firn first needs to be heated by refreezing until the melting point is reached is circumvented. The radar reflection horizon, as observed on the Greenland ice sheet in April 2011 [Forster *et al.*, 2013], represents the upper boundary of the liquid water body, and it intersects annual isochron layers, indicating that percolation is indeed heterogeneous, at least in part. First of all, preferential flow transports meltwater more quickly from the surface to the bottom of the firn layer (the firn-ice interface) and thus, less water remains stored in the firn. Secondly, the water that is held in the firn can refreeze more quickly because the liquid water in the pipes will be surrounded by cold firn that can accommodate latent

heat release by refreezing. These two arguments suggest that our model predicts the existence of a firn aquifer in a wider range of climate conditions than what may occur in real, preferential flow-dominated firn. The existence of preferential flow may also explain why the liquid water is found at depths that are generally greater (5–50 m with a mean depth of 23 m, *Forster et al.* [2013]) than the depth of the modelled firn aquifer (~10 m).

However, the conceptual framework explaining firn-aquifer formation does not depend on the percolation type. Low-accumulation sites cannot provide sufficiently deep pore space to store liquid water, regardless of the nature of meltwater percolation. For very high accumulation rates, sufficient cold content is available to absorb the latent heat released by refreezing, irrespective of how the water arrived at depth.

Observations by *Forster et al.* [2013] suggest that water exceeding the capillary storage capacity moves horizontally down the hydraulic gradient until it finds a crevasse or englacial channel where it is drained. Moreover, observed meltwater-flooded firn has densities significantly higher than the ice density [*Koenig et al.*, 2013]. These observations are not in line with two of our model assumptions, namely (1) that no more water storage is possible beyond the capillary storage capacity; and (2) that runoff at the firn-ice interface happens immediately. As a consequence, real firn aquifers may consist of firn flooded beyond its capillary storage capacity. As an important implication, the modelled decrease in firn-aquifer volume for increasing accumulation rate may not be seen in real firn.

In firn-aquifer regions, surface meltwater percolates into and is stored in the firn as opposed to being routed across the surface through supraglacial lakes and streams. Since the formation of these relatively dark supraglacial lakes and streams provides a strong

albedo feedback, the evolution of firn-aquifer regions in a warming climate is likely to differ from that of non-aquifer regions. Furthermore, firn aquifers potentially delay or preclude the transport of surface meltwater to the hydrological system in and under the ice sheet, meaning that there is no or little influence of surface melt on the ice dynamics. Also, the idea of catastrophic, jökulhlaup-like firn-aquifer drainage has been coined by *Koenig et al.* [2013], potentially affecting the rate at which Greenland meltwater contributes to sea-level rise. Thus, both surface mass balance and ice-dynamical models should discriminate between regions with and without firn aquifers, or at least more in general, between low- and high-accumulation regimes.

Acknowledgments. The authors are grateful for the constructive comments of two anonymous reviewers. Clément Miège (Univ. of Utah) is thanked for his help with the Operation Ice Bridge flight lines. Graphics were made using the NCAR Command Language (version 6.1.3, 2013). This research was carried out with financial support from the Netherlands Polar Programme (NPP) grant no. BN.000284, provided by the Netherlands Institute for Scientific Research (NWO).

References

- Arthern, R. J., D. G. Vaughan, A. M. Rankin, R. Mulvaney, and E. R. Thomas (2010), In situ measurements of Antarctic snow compaction compared with predictions of models, *J. Geophys. Res.*, *115*(F3), doi:10.1029/2009JF001306.
- Benson, C. S. (1962), Stratigraphic studies in the snow and firn of the Greenland ice sheet, *SIPRE Research Report 70*.

Braithwaite, R. J. (1985), Calculation of degree-days for glacier-climate research, *Z. Gletscherkd. Glazialgeol.*, *20*, 1–8.

Coléou, C., and B. Lesaffre (1998), Irreducible water saturation in snow: experimental results in a cold laboratory, *Ann. Glaciol.*, *26*, 64–68.

Forster, R. R., et al. (2013), Perennial liquid water discovered in Greenland firn layer, *Nat. Geosci.*, *accepted*.

Harper, J., N. Humphrey, W. T. Pfeffer, J. Brown, and X. Fettweis (2012), Greenland ice-sheet contribution to sea-level rise buffered by meltwater storage in firn, *Nature*, *491*, 240–243, doi:10.1038/nature11566.

Humphrey, N. F., J. T. Harper, and W. T. Pfeffer (2012), Thermal tracking of meltwater retention in Greenland's accumulation area, *J. Geophys. Res. (F)*, *117*(F01010), doi: 10.1029/2011JF002083.

Koenig, L. S., C. Miège, R. R. Forster, and L. Brucker (2013), Initial in situ measurements of perennial meltwater storage in the Greenland firn aquifer, *Geophys. Res. Lett.*, doi: 10.1002/2013GL058083.

Ligtenberg, S. R. M., M. M. Helsen, and M. R. van den Broeke (2011), An improved semi-empirical model for the densification of Antarctic firn, *The Cryosphere*, *5*, 809–819, doi:10.5194/tc-5-809-2011.

Marsh, P., and M.-K. Woo (1984), Wetting front advance and freezing of meltwater within a snow cover 1. observation in the Canadian Arctic, *Water Resour. Res.*, *20*(12), 1853–1864.

The NCAR Command Language (Version 6.1.3) [Software]. (2013). Boulder, Colorado: UCAR/NCAR/CISL/VETS. doi:10.5065/D6WD3XH5.

Selmes, N., T. Murray, and T. D. James (2011), Fast draining lakes on the Greenland Ice Sheet, *Geophys. Res. Lett.*, *38*(L15501), doi:10.1029/2011GL047872.

Van Angelen, J. H., J. T. M. Lenaerts, S. Lhermitte, X. Fettweis, P. Kuipers Munneke, M. R. van den Broeke, E. van Meijgaard, and C. J. P. P. Smeets (2012), Sensitivity of Greenland Ice Sheet surface mass balance to surface albedo parameterization: a study with a regional climate model, *The Cryosphere*, *6*, 1175–1186, doi:10.5194/tc-6-1175-2012.

Van den Broeke, M. R., C. Bus, J. Ettema, and P. Smeets (2010), Temperature thresholds for degree-day modelling of Greenland ice sheet melt rates, *Geophys. Res. Lett.*, *37*, L18,501, doi:10.1029/2010GL044123.

Accepted Article

Accepted Article

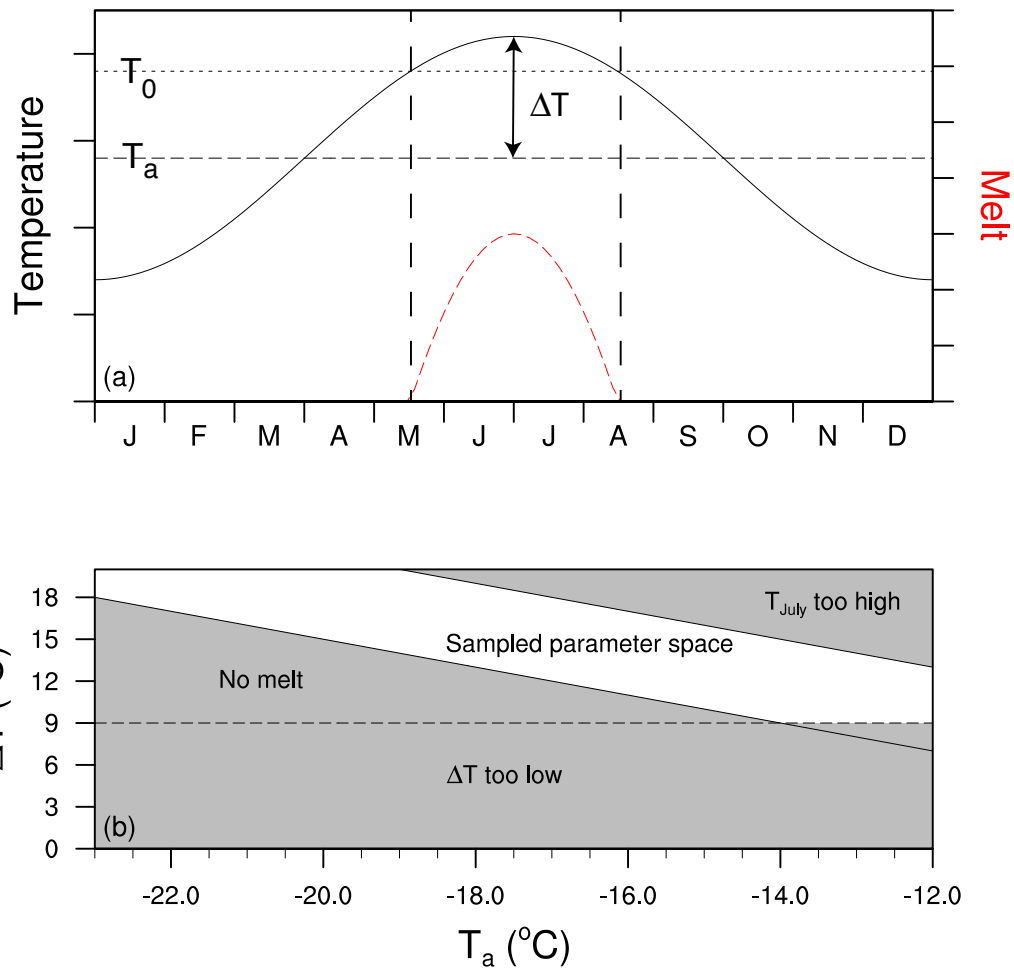


Figure 1. (a) Schematic picture of idealised surface temperature forcing T and surface melt flux M . T_a (lower dashed line) is the mean annual temperature, ΔT is the annual temperature amplitude, and T_0 (upper dashed line) is the temperature threshold for the positive degree-day calculation of melt. The vertical dashed lines mark the time period in which $T \geq T_0$. Melt M is shown in red with corresponding right Y-axis; (b) Overview of the surveyed parameter space in a $\{T_a, \Delta T\}$ -cross section. The white area represents the parameter space that we explore in this study.

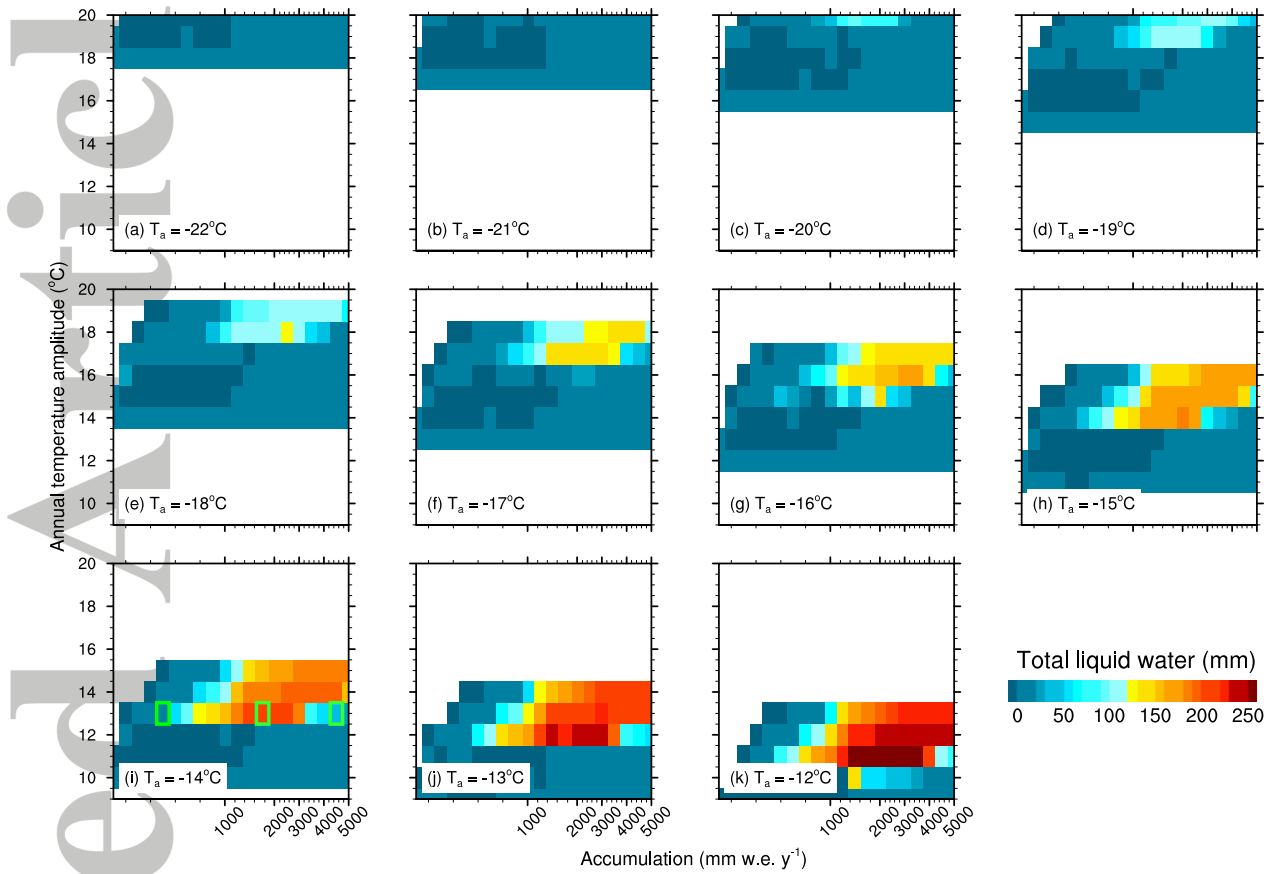


Figure 2. Vertically integrated water column (or total liquid water) (mm) at the end of winter (1 March), as a function of accumulation flux \dot{b} (X-axis), annual temperature amplitude ΔT (Y-axis), and annual mean temperature (the number indicated in the panel label), ranging from -22°C (panel a) to -12°C (panel k). The green rectangles in panel (i) indicate the climatic conditions of the firn profiles in Figure 3.

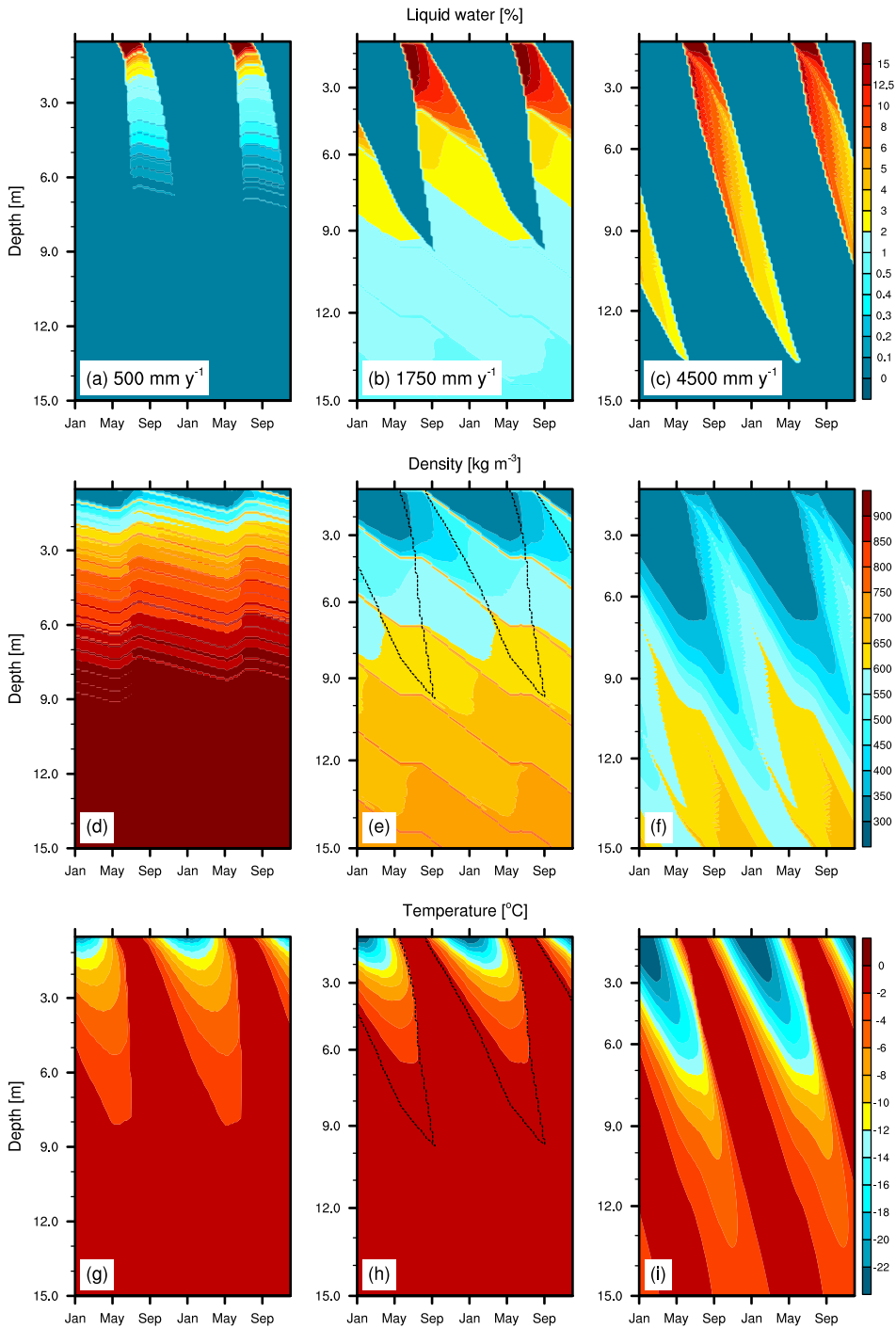


Figure 3. Two-year vertical profiles of liquid water content (in mass-%), density, and temperature, for identical surface temperature climate ($T_a = -14^\circ\text{C}$, $\Delta T = 13^\circ\text{C}$), and annual accumulation rates of (a),(d),(g) 500 mm w.e. y^{-1} ; (b),(e),(h) 1750 mm w.e. y^{-1} ; and (c),(f),(i) 4500 mm w.e. y^{-1} . Note the irregularly spaced color scale for panels (a)–(c). The 0%-contour of liquid water content from panel (b) is shown as a dashed line in panels (e) and (h) for visual guidance.

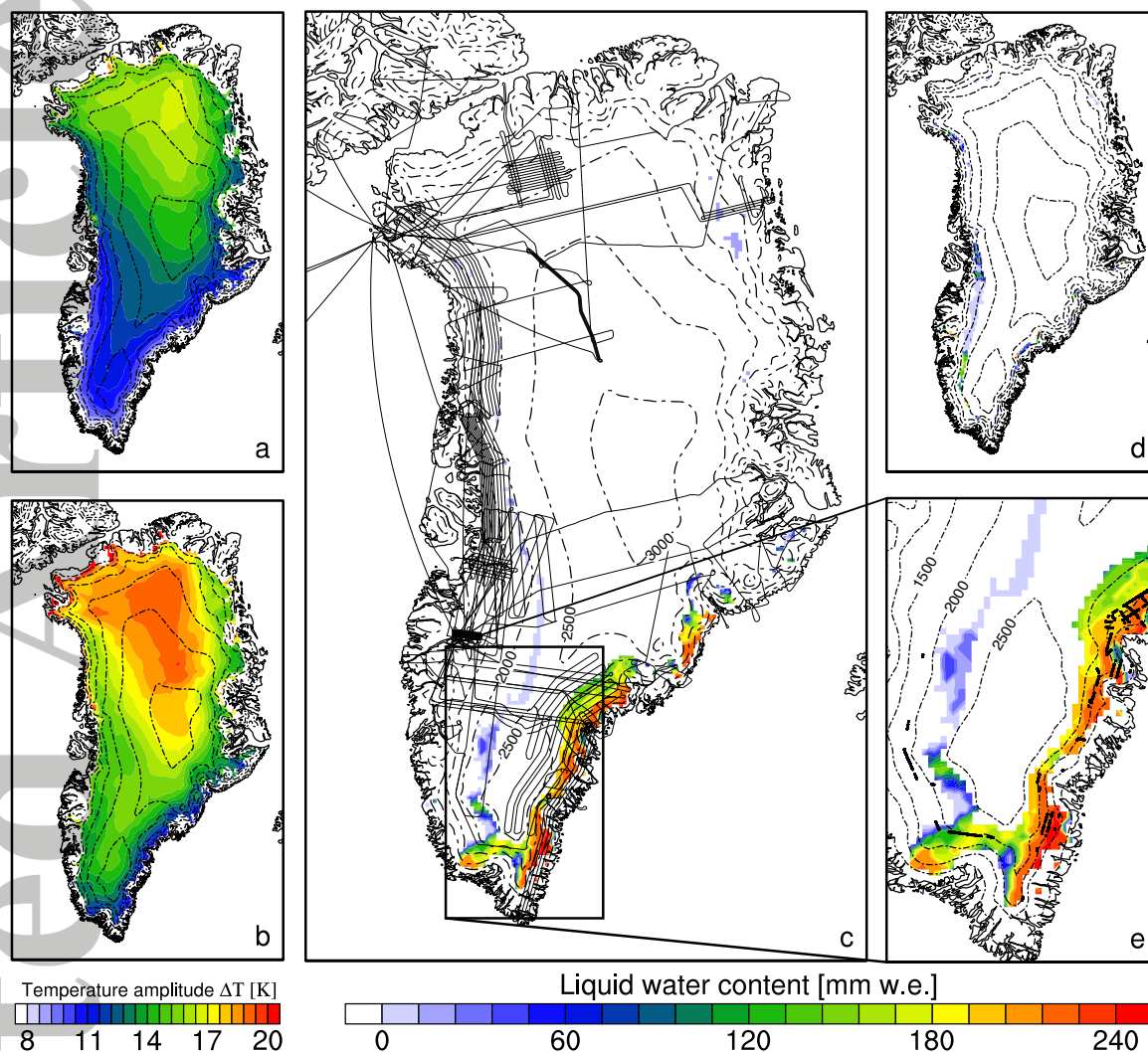


Figure 4. Liquid-water parameterization over the Greenland Ice Sheet based on temperature and accumulation fields from RACMO2. Labels and dash-dotted lines indicate height contours at 500 m intervals. (a) Temperature amplitude defined as the difference between the mean January and July temperature (in K); (b) Temperature amplitude defined as twice the winter-season temperature amplitude (in K); (c) Parameterized liquid water content (mm w.e.) using the temperature amplitude defined in panel b. All Operation Ice Bridge radar flight lines are drawn in thin solid black; (d) As in panel c, but with the temperature amplitude defined in panel a; (e) Inset over southeast Greenland, with data from c. Thick black dots indicate the Operation Ice Bridge-observed locations of firn aquifers.